World Academy of Science, Engineering and Technology
International Journal of Computer and Information Engineering
Vol:15, No:9, 2021

OILU Tag: A Projective Invariant Fiducial System

Youssef Chahir, Messaoud Mostefai, Salah Khodja

Abstract**—**This paper presents the development of a 2D visual marker, derived from a recent patented work in the field of numbering systems. The proposed fiducial uses a group of projective invariant straight-line patterns, easily detectable and remotely recognizable. Based on an efficient data coding scheme, the developed marker enables producing a large panel of unique real time identifiers with highly distinguishable patterns. The proposed marker Incorporates simultaneously decimal and binary information, making it readable by both humans and machines. This important feature opens up new opportunities for the development of efficient visual human-machine communication and monitoring protocols. Extensive experiment tests validate the robustness of the marker against acquisition and geometric distortions.

Keywords**—**Visual marker, projective invariants, distance map, level set.

I. Introduction

THE technological advances in the field of digital imaging techniques and systems enabled the development of high-performing virtual reality [1], [2] and autonomous navigation applications [3], [4]. These are based on efficient use of fiducial visual markers placed within their workspaces [5], [6]. There are many conceptions of visual markers in the literature (Fig. 1). Most of them are part of the square marker family (Fig. 1 (a)), which use 2D binary matrices to represent various patterns [7]-[9]. Each marker groups together a set of small regions (pixel or groups of pixels), to which a binary information is attributed. Since these are dot-matrix markers, any acquisition (lighting, noise etc.) or geometrical distortions will seriously diminish the recognition performances, and induce inter-marker confusion [10], [11]. A second group of circular markers is developed [12], [13]. The last one (Fig. 1 (b)) allows precise localization and is less sensitive to noise. Unfortunately, their performances are achieved at the expense of their computation complexity and limited information-coding capacity [14]. Another type of doted [15] and line based [16] projective invariant markers is developed (Figs. 1 (c), (d)). Even if they allow rapid and accurate detection, the last generate limited the markers libraries size.

Recently a new numbering system called OILU system has been developed and a dedicated patent was lately filled [17]. It associates basic (O, I, L and U) forms to decimal digits and allows producing various numbers with highly distinguishable patterns. The objective of this short paper is to show the effectiveness of such system in the development of efficient visual markers, less computational and robust to the well-known distortions.

M. M. is with the MSE Laboratory of Bordj Bou Arreridj University, BBA, 34000, Algeria (corresponding author, phone: 213-772-358-519; e-mail: m.mostefai@univ-bba.dz).

The remainder of this paper is structured as follows. Section II sets out the OILU system basics. Section III presents the development of visual OILU markers and shows their advantages. In Sections IV and V, the localization and the identification of the developed markers are described and software validated. Finally, Section VI concludes this paper.

II. Proposed System Basics

The proposed system is basically inspired from the human body anatomy [18], which is structurally composed of a head represented with "O" symbol, a spinal column represented with "I" symbol, and both upper and lower limbs represented with "L" and "U" symbols (Fig. 2 (a)). We all know that human body biomechanics is more complex than this [19], but in our case, these basic forms are largely sufficient for the construction of an efficient decimal numeration system. The latter is composed of 10 symbols, which are generated as follows: the first four symbols {O, I, L and U} represent respectively digits zero, one, two and three. The rest of the symbols are obtained by successive rotations (quarter counterclockwise) of the two basic symbols L and U (Fig. 2 (b)). Rotating symbols affectation is fixed according to their orientation (Fig. 2 (c)). As can be seen, the symbol O is represented with four segments, the symbol I with one segment, the segment L with two segments and finally, the segment U with three segments.

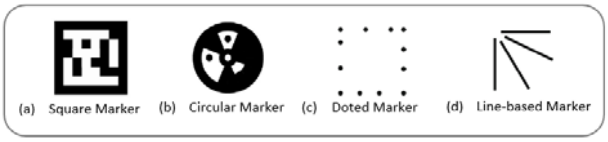

Fig. 1 Example of Visual Markers

The main interesting point with this symbolism is that it allows superimposing symbols in pyramidal form without losing the value of constructed numbers. Fig. 3 (a) presents a pyramidal composition of the decimal number 4670. The lecture sense is from the outside to the inside. Unlike the classical numeral decimal symbolic, the OILU symbolic allows to see a number as an object with its four facets. Indeed, we can extract from each point of view a different number value. Thus, a group of related numbers is formed: 4670 – 2450 – 8230 – 6890. Note that any facet's value allows deducing the other facets values. Multi facets numbers have interesting applications in the large field of data processing, but in our case, they are exploited for the design of new efficient square OILU markers.

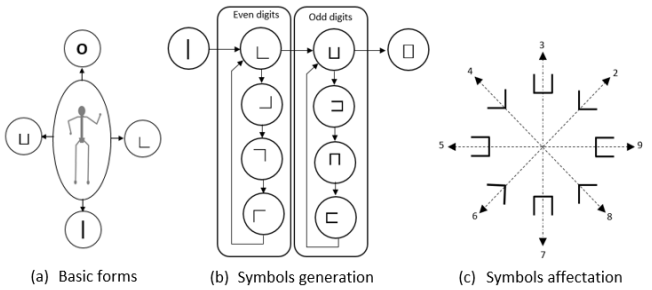

Fig. 2 OILU Symbols Generation

III. Square Markers Design

Developed markers are composed of regularly concentric segments. The paths are orderly disposed from the center to the outside. Moreover, this topology allows having the same distance between neighboring segments. The placement of symbols gives a hierarchy of contours as Parallel-Edges. These are designed according to the surrounding space characteristics: black segments on white background or white segments on black background (Fig. 3 (b)).

Conceptually, proposed OILU markers present several advantages. Amongst these, we have:

- ✓ OILU markers are composed of a set of projective invariant line segments [15], [16].
- ✓ OILU markers are highly distinguishable even if they have a difference of only one segment/bit (Hamming distance =1). This is the case for example with the two neighboring markers presented in Fig. 3 (c). Indeed, according to OILU symbols' structure (Fig. 3 (d)) and codification (Fig. 4), these markers are represented with the following codes: (a) → (1101 1100 1011 1101) and (b) → (1101 1100 1011 1111).
- ✓ Generated OILU Marker library size depends on the number of embedded symbols. If N is the number of embedded symbols, the number of unique markers U_N is equal to $10^N/4$. For N = 4 for example, the number of possible markers is equal to 2500, which is largely sufficient for applications requiring a huge number of unique markers.

IV. Markers Detection and Identification

To ease marker detection, the visual OILU markers are printed on a white background with a black outline square, or on a black background with a white outline square. The captured images are grayscale converted and then binarized. A cleanup operation is applied to remove all connected components that have less than a certain number of connected pixels. The marker boundaries are then detected and the region of interest is cropped. The following step consists on generating embedded code from groups of parallel-line segments. Such task can be considered as a geometrical problem, that can be solved with space filling and distance maps methods [20]. As can be seen, the proposed markers topology is similar to Fermat's spirals [21]. The latter has many interesting properties that can be exploited to solve difficult geometric problems, such as markers identification, which in our case, is a pure geometrical pattern recognition problem.

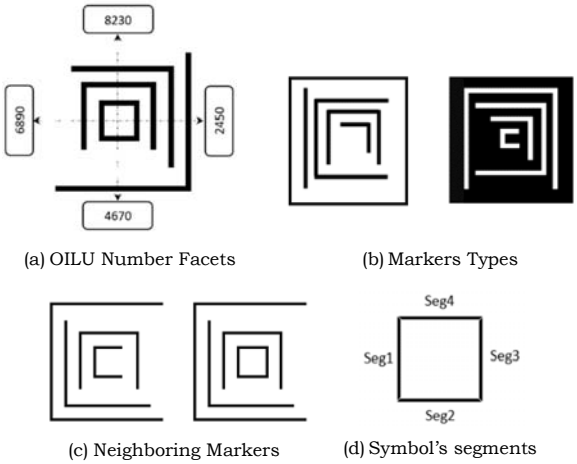

Fig. 3 Markers Presentation

Decimal	OILU Symbol	Symbol's components			
		Seg1	Seg2	Seg3	Seg4
0	□	1	1	1	1
1	⌶	1	0	0	0
2	⌞	1	1	0	0
3	⌴	1	1	1	0
4	⌟	0	1	1	0
5	⌑	0	1	1	1
6	⌝	0	0	1	1
7	⌐	1	0	1	1
8	⌜	1	0	0	1
9	⌐	1	1	0	1

Fig. 4 Symbols Codification

In this paper, we used a variant of Fermat spirals as a 2D filling model. The idea is to use a double spiral filling curve where the inside and outside are connected by a straight line. The placement of OILU symbols (representation of edges by segments) gives a hierarchy of contours as parallel-edges, see Figs. 5 (a) and (b). The level-set method [22], [23] offers a more straightforward solution for offset geometric structures to generate distance maps. In this method, the quadrilateral border (Ω) is represented by an implicit function Φ, which has the following properties: the function has a null value on the boundaries, negative values in the inner region, and positive values in the outer regions (as illustrated in Fig. 5 (c)). The signed function can be defined as:

$$\Phi(\mathrm{p}) = \begin{cases} -d(p) = W & if\ p\ \in \Omega \\ 0 & if\ p\ \in \partial\Omega \\ d(p) = -W & if\ p\ \notin \Omega \end{cases}$$

where d(.) is a distance function.

From an arbitrary quadrilateral border (Ω), we can localize and reconstruct others quadrilaterals, because this approach can smoothly propagate the boundaries inside or outside the square

for generating constant offset parallel contours patterns [24], especially when $|\nabla\Phi| = 1$.

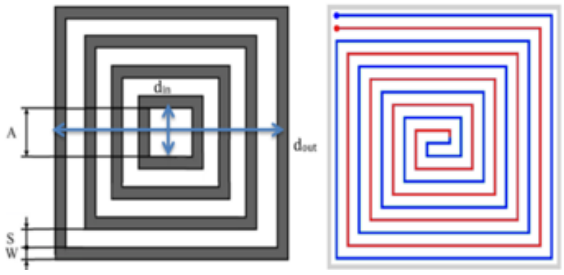

(a) OILU Markers Topology (b) Fermat Spirals Topology

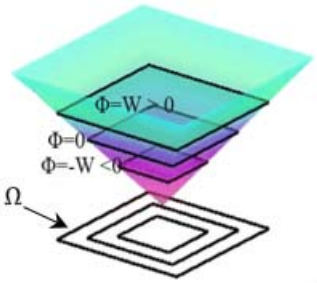

(c) Link between Squared distances Transform and Level Sets

Fig. 5 Markers Distance Map Generation

Once the marker distance map is generated, an inward propagation is performed to label the pixels inside the quadrilateral, according to the level set or turns (see Fig. 6).

To extract the embedded code, we do the following:

1. Divide the main quadrilateral into four triangles, obtained from the diagonals. The analysis of a triangle allows to know if the OILU segments are present or not.
2. For each triangle we do the following:

- Check whether a labeled point lies inside a triangle or not.
- Count the labeled points inside a triangle. If the number of points surpasses a given threshold, a segment is considered to be present. It will be represented by '1', otherwise '0'.

V. Preliminary Experimental Tests

Tests were performed on synthetic and real markers. For this purpose, a synthetic OILU database (composed of 20,000 markers) is generated automatically using a dedicated OILU markers generator program (Fig. 7 (a)). Real markers (Fig. 7 (b)) are acquired using an ordinary 640x480 video surveillance camera (TL-SC3230N), presented in Fig. 7 (c). Both types of markers are freely downloadable at [25].

First tests are carried on synthetic markers which are gradually degraded using several well-known distortions (additive noise, blur and radial distortion). Obtained robustness tests are presented in Fig. 8. As can be seen, the markers identification scheme demonstrated satisfactory results even with high levels of distortions. This is mainly due to the fact that segments labeling is based on a pre-established distance map.

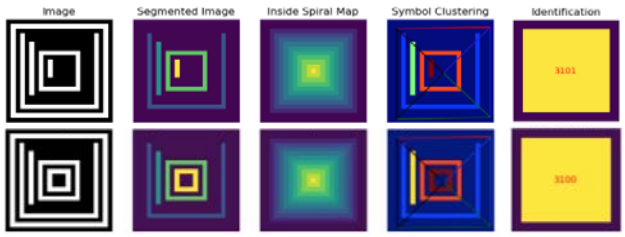

Fig. 6 OILU Marker Identification

The second series of tests are performed in a real environment using two different size markers M1 (12 x 12 cm) and M2 (6 x 6 cm). Initially, we evaluate the impact of the marker to camera distance on the performances of marker detection and recognition. The camera was positioned at different distances from approximately 0.5 m to 6 m. The distance range at which the marker was reliably detectable and identifiable was between 0.5 m and 3 m for the marker M2, and extended to 5 m for the marker M1(Fig. 9).

The third test concerns the robustness to viewing angle (Fig. 10). OILU markers were acquired with variable angles of view, ranging from approximately 5° to 30°. Marker identification was successful only for angles superior than 10°. Below this angle, the segments are very close, which makes identification very difficult. We also tested the algorithm in difficult lighting conditions. As can be seen (Fig. 11), below a certain lighting level (20 Lux), identification becomes impossible.

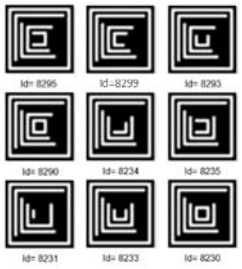

(a) Synthetic OILU Markers

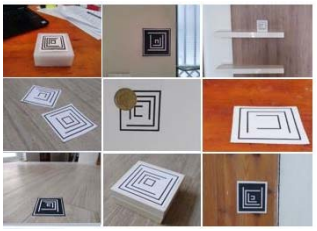

(b) Real OILU Markers

(c) Distance and Viewing Angle Test Dispositive

Fig. 7 Synthetic and Real Markers Generation

The last test consists on evaluating the impact of occlusion by overlapping markers with circles (money pieces). Two situations of occlusion are presented in Fig. 12. As long as a segment is not completely covered (Figs. 12 (a) and (b)), the marker is successfully identified. Otherwise, the identification fails. Indeed, only parts of a segment need to be visible in order

to extract its parameters. However, in case of central occlusion (Fig. 12 (c)), and more particularly, where a complete segment is occluded, the authentication fails.

The experiments have been performed on a typical Mac Book, equipped with a 2.9 GHz Intel Core i5 processor and 8 Go of RAM. Detection and identification performances are evaluated by computing the processing time for marker detection and identification. The latter is around 40 ms. This result shows that even if Level Set methods are efficient, they remain computationally expensive. We are actually working on a faster method, which allows real-time identification of the targeted marker. At this stage, we continue to improve the performances of this method, especially against occlusion. A demonstration of the initial version is available at [25].

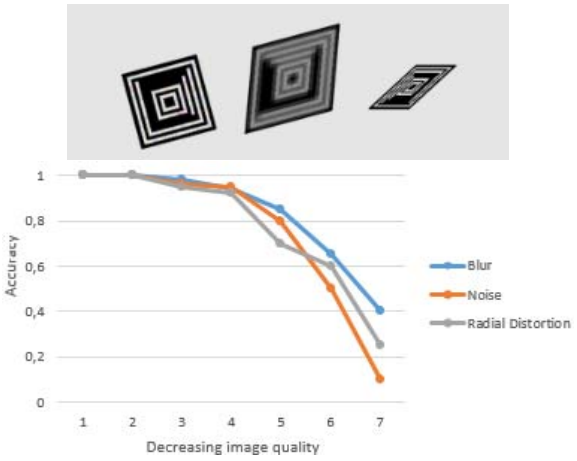

Fig. 8 Robustness to distortions

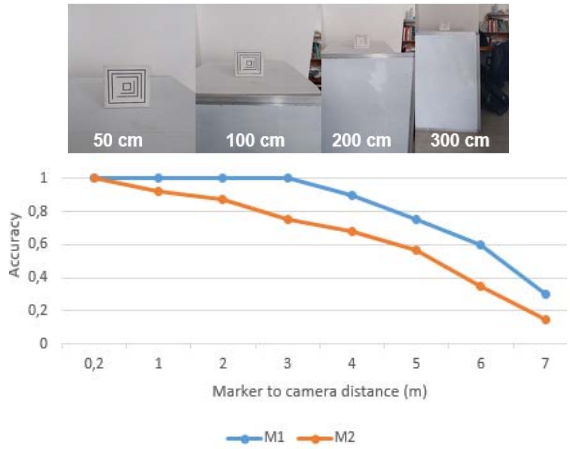

Fig. 9 Front detection and identification

VI. Conclusion

We have presented the development of a visual 2D marker based on the OILU numbering system. The latter uses simple patterns and allows generating a rich and highly distinguishable set of projective invariant markers. Based on Level Set methods, the developed identification scheme effectively exploits the spiral topology of OILU markers to perform accurate marker labeling and recognition, but at the expense of computing time.

Presented preliminary tests aim at validating the OILU marker functionality. However, deep comparative tests are required to accurately evaluate the OILU marker's performances against leading state of the art markers. Additionally, software improvements are necessary to allow robust real-time identification and pose estimation.

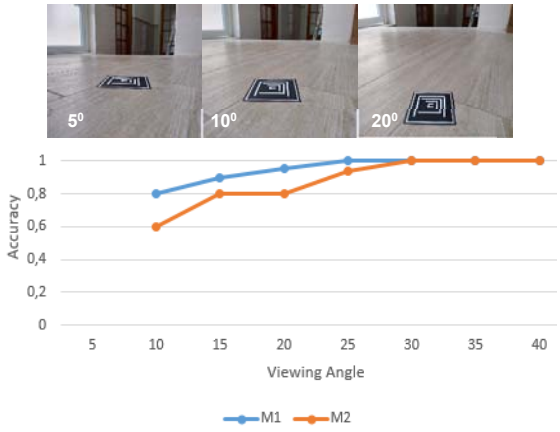

Fig. 10 Perspective Identification Accuracy

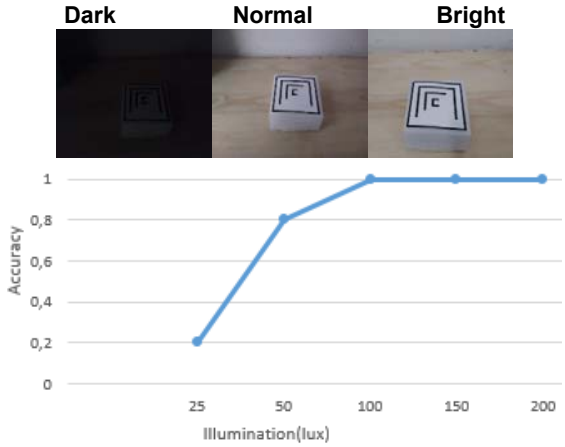

Fig. 11 Robustness to Lighting Changes

(a) (b) (c)

Fig. 12 Robustness to Occlusion

Proposed line-based OILU markers are human-machine readable fiducials, which combine efficiently the 1D and 2D barcodes technologies to gain in simplicity and robustness. These allow the production of a wide range of unique identifiers with highly differentiable patterns, thus providing new opportunities for the development of efficient human-machine visual communication and monitoring protocols. OILU markers are publicly available for tests via a dedicated web site

[25], which also provides examples of developed programs. These are subject to improvements.

REFERENCES

[1] Sarmadi H, et al., 3D Reconstruction and alignment by consumer RGB-D sensors and fiducial planar markers for patient positioning in radiation therapy, Computer Methods and Programs in Biomedicine. 2019.
[2] F.-E. Ababsa and M. Mallem, Robust camera pose estimation using 2D fiducials tracking for real-time augmented reality systems, in Proc. ACM SIGGRAPH Int. Conf. (VRCAI), 2004, pp. 431-435.
[3] N. Mohammad et al., Automated Localization of UAVs in GPS-Denied Indoor Construction Environments Using Fiducial Markers, 2018.
[4] J. Wubben et al., Accurate Landing of UAV Using Ground Pattern Recognition. Electronics 2019, 8, 1532.
[5] E. Olson, AprilTag: A robust and flexible visual fiducial system," IEEE International Conference on Robotics and Automation, Shanghai, 2011, pp. 3400-3407, 2011.
[6] J. Čejka et al., Detecting Square Markers in Underwater Environments. Remote Sens. 2019, 11, 459.
[7] G.C. La Delfa et al., Performance analysis of visual markers for indoor navigation systems, Frontiers Inf Technol Electronic Eng 17, 730–740 (2016).
[8] P. Lightbody et al., An efficient visual fiducial localisation system, AC Review, 17 (3). pp. 28-37. (2017).
[9] S.M. Abbas et al., A. Analysis and Improvements in AprilTag Based State Estimation. Sensors 2019, 19, 5480, https://doi.org/10.3390/s19245480.
[10] P. Jin et al., Sensor fusion for fiducial tags: Highly robust pose estimation from single frame RGBD," 2017 IEEE/RSJ International Conference on Intelligent Robots and Systems (IROS), Vancouver, BC, 2017, pp. 5770-5776.
[11] A. Zea and U. D. Hanebeck, Refined Pose Estimation for Square Markers Using Shape Fitting, 22th International Conference on Information Fusion (FUSION), Ottawa, ON, Canada, 2019, pp. 1-8.
[12] T. Birdal et al., X-Tag: A Fiducial Tag for Flexible and Accurate Bundle Adjustment, Fourth International Conference on 3D Vision (3DV), Stanford, CA, 2016, pp. 556-564, doi: 10.1109/3DV.2016.65.
[13] L. Calvet et al., Detection and Accurate Localization of Circular Fiducials under Highly Challenging Conditions, 2016 IEEE Conference on Computer Vision and Pattern Recognition (CVPR), Las Vegas, NV, 2016, pp. 562-570.
[14] A. C. Rice et al., Cantag: an open source software toolkit for designing and deploying marker-based vision systems, (PERCOM'06) Conference, Pisa, pp. 10-21.2006.
[15] F. Bergamasco et al., Pi-Tag: a fast image-space marker design based on projective invariants, Machine Vision and Applications 24, 1295–1310 (2013). https://doi.org/10.1007/s00138-012-0469-6.
[16] R. van Liere and J. D. Mulder, Optical tracking using projective invariant marker pattern properties, IEEE Virtual Reality Proceedings, Los Angeles, CA, USA, 2003, pp. 191-198, doi: 10.1109/VR.2003.1191138.
[17] M.Mostefai and S.Khodja, OILU Symbolic, US patent application No 63-424, 2020.
[18] D. Gentry Steele and Claud A. Bramblett, The Anatomy and Biology of the Human Skeleton, Texas A&M University Press, 1988.
[19] A. Sophie et al., Action recognition based on 2D skeletons extracted from RGB videos, MATEC Web Conf. 277 02034 (2019), DOI: 10.1051/matecconf/201927702034.
[20] Pedro F. Felzenszwalb and Daniel P. Huttenlocher, Distance Transforms of Sampled Functions, Theory of Computing, Volume 8(19), pp. 415-428, 2012.
[21] M.G. Óscar et al., 2D array design based on Fermat spiral for ultrasound imaging, Ultrasonics. 50. 280-9. 10.1016/j.ultras.2009.09.010.
[22] S. Osher, J. Sethian, Fronts Propagating with Curvature Dependent Speed: Algorithms Based on Hamilton-Jacobi Formulations, Jour Computing Phys. 79, pp.12-49, 1988.
[23] D. Adalsteinsson, J. Sethian, A Fast Level Set Method for Propagating Interfaces, Jour. Computing Phys., Vol. 118, pp. 269-277,1995.
[24] Y. Xiong et al., Process planning for adaptive contour parallel tool path in additive manufacturing with variable bead width, Int J Adv Manuf Technol 105, 4159–4170 (2019). https://doi.org/10.1007/s00170-019-03954-1.
[25] OILU code web site: http://oilucode.net